Novel Subharmonically Pumped Mixer Incorporating Dual-Band Stub and In-Line SCMRC

Tsz Yin Yum, *Student Member, IEEE*, Quan Xue, *Member, IEEE*, and Chi Hou Chan, *Fellow, IEEE*

***Abstract*—A subharmonically pumped (SHP) mixer with very low conversion loss is proposed. The mixer employed the newly developed spiral compact microstrip resonant cell (SCMRC) and compact dual-band stub (DBS). Incorporating the in-line SCMRC and DBS into a second SHP mixer, we can provide proper terminations for the IF, RF, and local-oscillator (LO) signal simultaneously in addition to all major unwanted mixing products, leading to a unique low conversion-loss design. Our SHP mixer with a measured 3.9-dB single-sideband (SSB) down-conversion loss at 11.6-GHz RF signal outperforms typical designs of 8–12 dB, and represents a state-of-the-art performance for a planar X-band harmonic mixer. With a broad-band operation, our mixer shows an SSB down-conversion loss of less than 8.2 dB from 9 to 12.8 GHz. Moreover, the measured LO–RF isolation is better than 45 dB for LO frequency ranges of 4–5.8 GHz. Large-signal two-tone measurements reveal an excellent linear response of the working prototype, showing 7.5 dBm and 52 dB for the 1- dB power compression point and spurious-free dynamic range, respectively.**

***Index Terms*—Dual-band stub (DBS), 1-dB power compression point (P1dB), quasi-lumped component, spiral compact microstrip resonant cell (SCMRC), subharmonically pumped (SHP) mixer.**

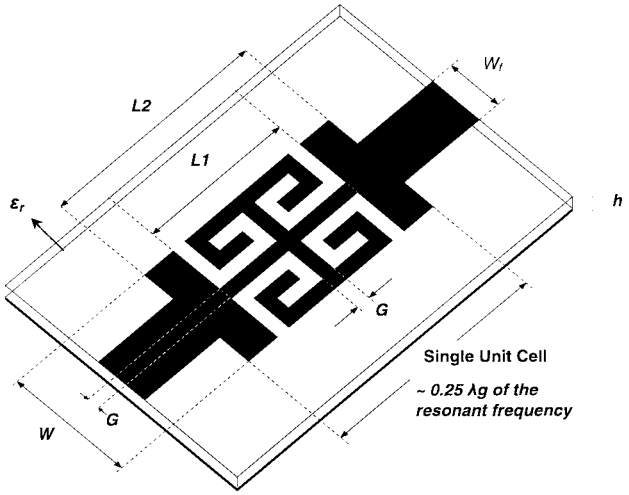

Fig. 1. Three-dimensional view of the SCMRC structure. $h = 0.254$ mm, $\varepsilon_r = 2.2$, $W_f = 0.8$ mm, $W = 1.8$ mm, $G = 0.2$ mm, $L1 = 2.2$ mm and $L2 = 3.2$ mm.

I. Introduction

SUB-HARMONICALLY pumped (SHP) mixers using an antiparallel Schottky diode pair pumped by two, four, or more even multiples of the lower frequency local oscillators (LOs) are very attractive for low-cost microwave and millimeter-wave systems. However, the conversion loss of SHP mixers is usually much higher than that of fundamental pumped counterparts and many papers have been devoted to their performance improvement [1]–[9]. A wide-band second subharmonic mixer monolithic microwave integrated circuit (MMIC) with 12.9-dB conversion loss is proposed in [6]. In addition, a 60-GHz uniplanar MMIC fourth subharmonic mixer has also been realized in finite ground coplanar (FGC) waveguide technology [7], and a minimum conversion loss on the order of 14 dB has been achieved. Meanwhile, though a fundamental limitation of conversion loss on an even harmonic mixer of approximately 3.9 dB has been suggested in [8], only a 9.5-dB conversion loss is achieved experimentally. Consequently, it seems that designs of harmonic mixers with low conversion loss remain a great challenge. In [9], an excellent design methodology was proposed for subharmonic mixers; however, it is difficult to satisfy its state-of-the-art criteria when implemented with conventional circuits. Therefore, only a 9-dB conversion loss is obtained [9]. In this paper, we proposed a low conversion-loss SHP mixer design employing our novel spiral compact microstrip resonant cells (SCMRCs).

The compact microstrip resonant cell (CMRC), as proposed in [10], is a quasi-lumped circuit element that has similar characteristics of slow-wave and bandstop effect as the electromagnetic bandgap (EBG) [11]–[13]. Its compactness makes it suitable for various passive and active circuit applications [14]–[16]. Recently, we have proposed a new approach for terminating the mixing products in the fourth subharmonic mixer based on our novel CMRC structures, yielding a conversion loss of 6.1 dB at 35 GHz [17], in which two CMRCs are used to provide suitable terminations for different frequencies in the mixer according to the criteria of [9]. While we can improve the mixer performance significantly, the size of the mixer is inevitably increased due to the inclusion of the two CMRCs that are connected in series. To alleviate this difficulty, we introduce a new spiral CMRC that has a stronger slow-wave effect than the original one reported in [10].

With further size reduction capability of the SCMRC, a dual-band stub (DBS) can be realized. Such a DBS can be in the form of either open–open or open–short combinations. These DBSs provide more design flexibility in eliminating unwanted harmonics than the conventional quarter-wave stubs. Incorporating DBS and the in-line SCMRC into the SHP mixer, we can provide proper terminations for the IF, LO, RF, and major unwanted frequency mixing products simultaneously,

Manuscript received April 17, 2003. This work was supported by the Hong Kong Research Grant Council under Grant CityU 1237/02E. The work of T. Y. Yum was supported under a Sir Edward Youde Memorial Fellowship.

The authors are with the Wireless Communications Research Center, City University of Hong Kong, Kowloon, Hong Kong (e-mail: 50182327@student.cityu.edu.hk).

Digital Object Identifier 10.1109/TMTT.2003.820152

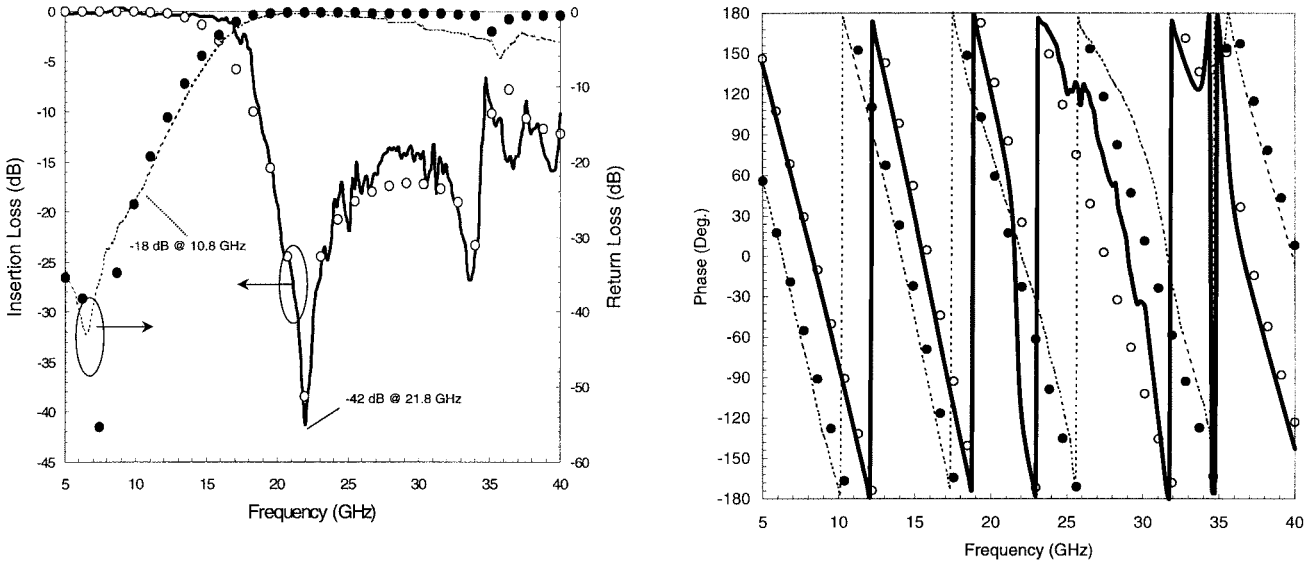

(a) (b)

Fig. 2. Scattering parameters for the SCMRC structure with: (a) magnitude in decibels. (b) Phase in degree. •: simulated S_{11}. · · ·: measured S_{11}. ∘: simulated S_{21}.—: measured S_{21}.

leading to a very low conversion-loss design without sacrificing the circuit size.

This paper is organized as follows. In Section II, the theory and design of the SCMRC is introduced with its corresponding scattering and phase characteristics. In addition, a practical open–open DBS with the SCMRC is presented. The design of a new second-order SHP mixer is discussed in Section III using the designed open-short DBS and in-line SCMRC. Performance of the proposed mixer is given in Section IV. As linearity is a common concern in modern communication systems, we also include measurement results in regard to the proposed mixer's intermodulation distortion (IMD) performance. Finally, conclusions and discussions are made in Section V.

II. SCMRC AND THE DESIGN OF DBS

A. Spiral CMRC

The CMRC in [10] exhibits slow-wave and bandstop characteristics. To further enhance the slow-wave effect for circuit size reduction, we propose a unique SCMRC structure, which is shown in Fig. 1. As can be seen from this figure, this SCMRC consists of four folded lines instead of four triangular pattern depicted in [10]. Without increasing the size, the folded pattern greatly enhances the inductance, while the coupling gaps between the lines increase the capacitance of the transmission line. The increases of line inductance and capacitance make the structure a slow-wave transmission line, which can significantly reduce the circuit layout. Also, the nonuniform increments of inductance and capacitance in the structure lead to multipoint resonance, which results in a wide bandstop effect. For matching purpose, the width of the cell (W) is carefully adjusted to attain 50-Ω characteristic impedance in order to compensate for the unbalanced change of inductance and capacitance while maintaining a low insertion loss over the passband region [18]. A demonstration circuit was simulated, fabricated, and measured. The circuit was on a Duroid5880 substrate with a relative permittivity of 2.2 and a height of 0.254 mm. Simulation was performed using *ENSEMBLE 6.0*.[1] Fig. 2(a) shows the simulation and measured S-parameters of the SCMRC structure. Here, a distinctive stopband has been observed from 19 to 36 GHz, which is approximately 68% (-10 dB) bandwidth. It can also be seen that by increasing the width W of the SCMRC from 0.8 mm, which is the width of a 50-Ω regular microstrip line, to 1.8 mm, the transmission performance ($S21$) in the low-pass region has a maximum insertion loss of 0.2 dB and the return loss is lower than -40 dB. The return loss in the stopband region is very close to 0 dB, indicating a negligibly small radiation loss.

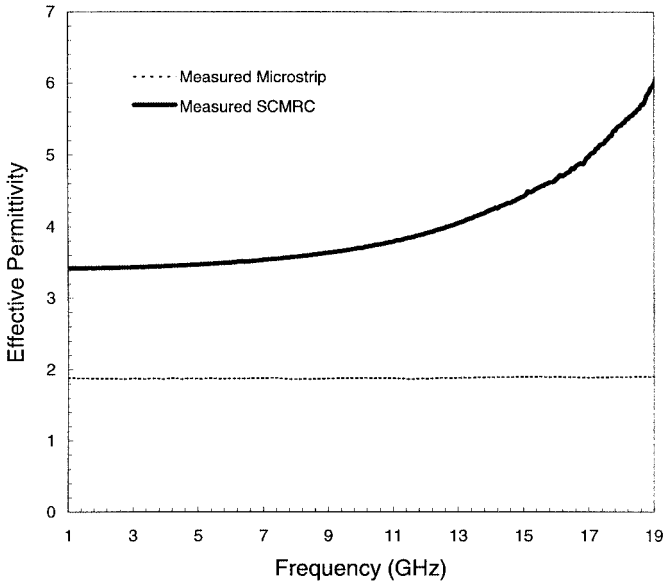

Fig. 3. Comparison of SWFs in terms of the effective permittivity for the proposed SCMRC structure and uniform microstrip line.

Fig. 2(b) reveals that the phase variation of S_{21} with frequency is quite linear, suggesting the proposed SCMRC is an excellent waveguiding structure. Fig. 3 reports the variation of the

[1]*ENSEMBLE* is a Trademark of Ansoft Inc., Pittsburgh, PA.

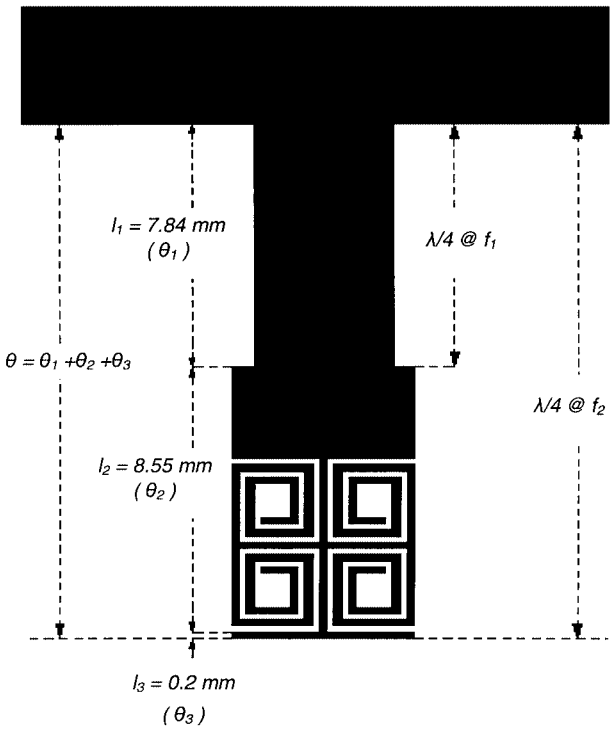

Fig. 4. Layout structure and operation concept of the open–open DBS.

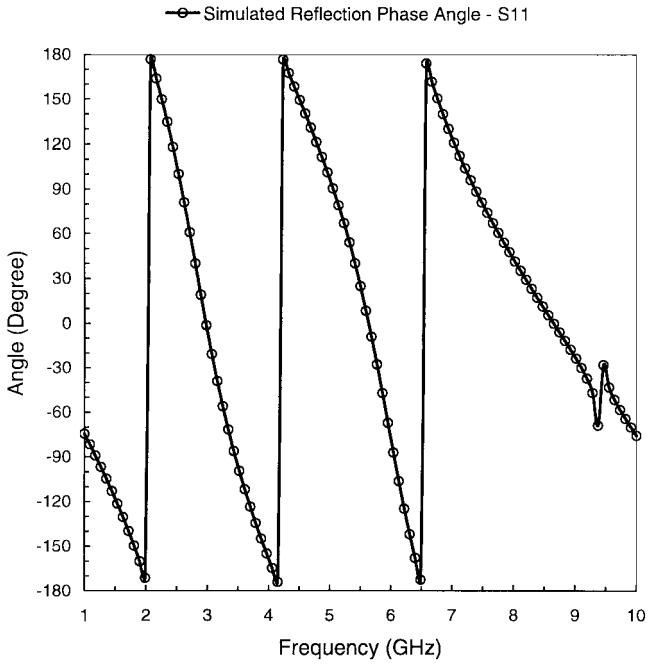

Fig. 5. Simulated reflection phase (S_{11}) looking into the dual-band resonator.

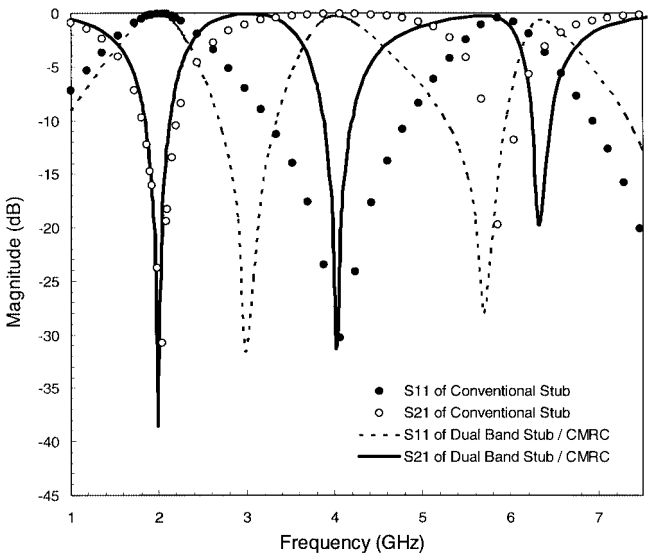

Fig. 6. Comparison of the scattering parameters (S_{11} and S_{21}) for the DBS and conventional quarter-wave stub.

slow-wave factor (SWF) in terms of the effective permittivity, with frequency. It can be seen that the uniform microstrip line shows an SWF of 1.88 in the passband region (e.g., 11 GHz), where the proposed SCMRC increases the SWF by 108% to 3.9 and is even better than 180% at the onset of the stopband around 18 GHz. Such an increase in the SWF shows that the proposed SCMRC is an excellent slow-wave transmission line, further validating the size-reduction capability of the proposed structure. In fact, increasing the number of turns in the spiral, making the SCMRC more compact and flexible, can further reduce the size of the SCMRC for circuitry design.

B. DBS

Using stub filters to suppress spurious harmonics is a common technique in designing microwave active circuits. In an SHP mixer, many open/short-stub networks are needed to provide the return paths and suitable terminations for major signals and other undesired mixing products [4]–[9]. However, when the number of signals and their spurious responses increases, extra stubs are usually required, occupying more area for the circuit layout. Due to size constraints, extra stubs and filters may not be easily added. Moreover, such stubs would have a great impact on the impedance matching of the diode pair, which results in an increase of the overall LO power requirement. In this section, the SCMRC is inserted into an open-circuit quarter-wave stub such that it not only reduces the size of the structure by the slow-wave effect, but also provides a well-controllable dual-frequency operation by its stopband characteristics. A brief demonstration of a DBS operated with open-open combination is discussed below.

Fig. 4 depicts an open-circuit DBS. To give a return path for two frequencies, say, f_1 and f_2 with $f_2 > f_1$, we must have both reflection phases of these frequencies looking into the quarter-wave resonator equal to $\pm 180^\circ$. The SCMRC in the stub is first designed to have a stopband at f_2, as well as a low-loss transmission in the f_1 region. We then tune θ_1 so that the reflection phase of terminating resonance at f_2 equal to $\pm 180^\circ$ for the return path. This is followed by tuning θ_3 so that the reflection phase of the terminating resonance satisfies the condition $\theta = \theta_1 + \theta_2 + \theta_3 = \pm 180^\circ$ for the return of f_1. By the above description, the operation of the DBS is as follows: the whole stub remains a quarter-wavelength long at the lower operating frequency f_1. On the other hand, due to the stopband characteristic of the SCMRC at the higher operating frequency f_2, the open circuit will be shifted to the location where the SCMRC begins.

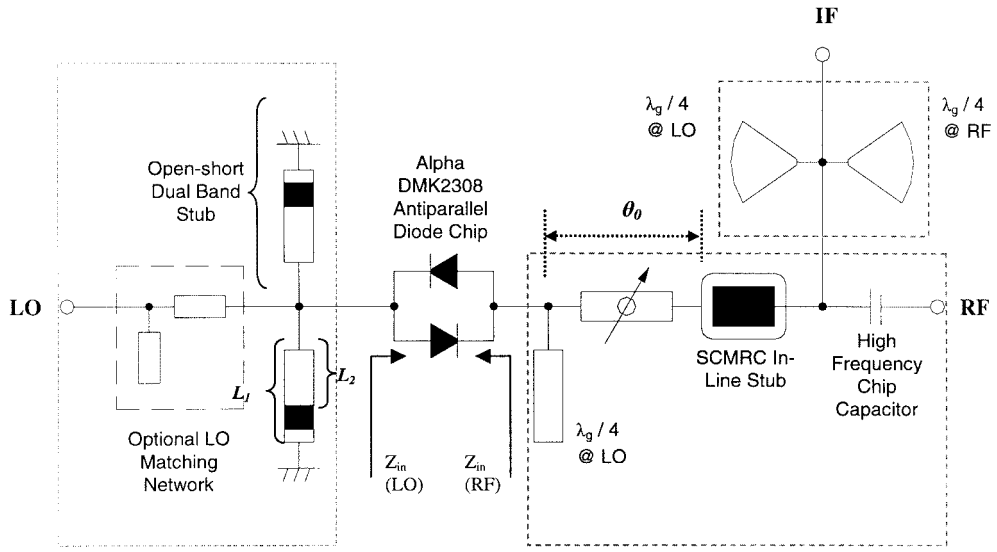

Fig. 7. Schematic diagram of the proposed second-order SHP mixer.

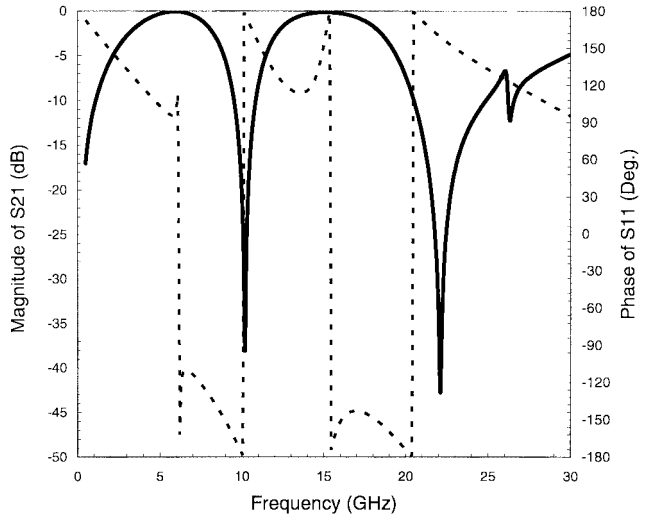

Fig. 8. Simulated scattering parameters for the LO network. —: magnitude of S_{21}. —: phase of S_{11} looking from the left terminal of the diode pair.

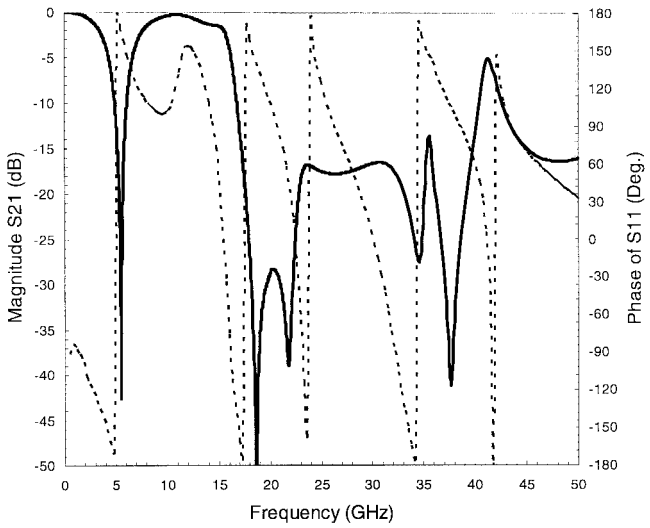

Fig. 9. Simulated scattering parameters for the RF network. —: magnitude of S_{21}. —: phase of S_{11} looking from the right terminal of the diode pair.

If the remaining upper section of the stub is also a quarter-wavelength long at the higher operating frequency f_2, the design of a dual-frequency open-circuit quarter-wave stub is achieved.

To study the effect of the spirals and for the ease of circuit fabrication, we have implemented the above approach in the design of a dual-band open-open quarter-wave stub operated at 2 and 4 GHz as an illustrative example. The substrate is Duriod5870 with a dielectric constant 2.94 and a thickness of 1.524 mm. Simulations were conducted using Ansoft's *ENSEMBLE* in order to determine the optimum design of the DBS on the given substrate. Fig. 5 first shows the simulated reflection phases looking into the stub. The dimensions of the stub are $l_1 = 7.84$ mm, $l_2 = 8.55$ mm, and $l_3 = 0.2$ mm. Due to the slow-wave effect, both 2 and 4 GHz have the reflection phases of the terminating resonance equal to $\pm 180^\circ$. For comparison, a conventional open-circuit quarter-wave stub centered at 2 GHz is fabricated and measured. Fig. 6 shows the measured S-parameters of both the DBS and conventional

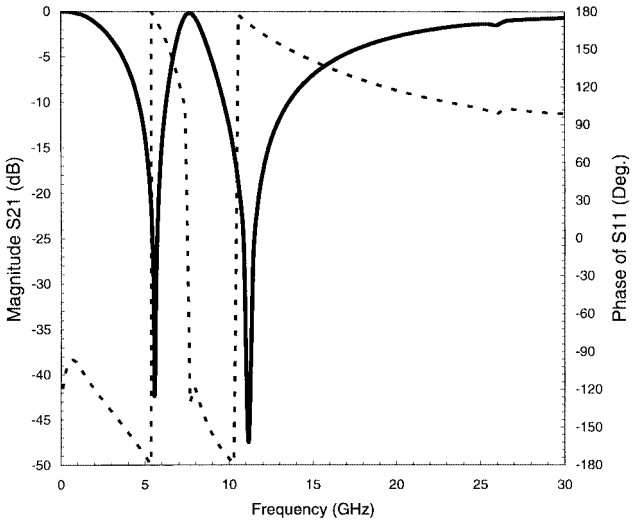

Fig. 10. Simulated scattering parameters for the IF network. —: magnitude of S_{21}. —: phase of S_{11} looking from the IF port.

TABLE I
ALPHA DMK2308 GaAs SCHOTTKY DIODE PARAMETERS

Saturation Current I_S (Amp)	Series Resistance R_S (Ω)	Ideality Factor n	Junction Cap. C_p (pF)	Built-in Voltage (eV)	Cut-off Freq. (GHz)	Reverse Breakdown Volt. (V)
5×10^{-13}	7.0	1.05	0.05	0.82	455	4.0

TABLE II
SIMULATION RESULTS OF THE PROPOSED SECOND-ORDER SHP MIXER

f_{LO} (GHz)	f_{IF} (GHz)	f_{RF} (GHz)	P_{LO} (dBm)	Conversion Loss (dB)	$Z_{in,LO}$ (Ω)	$Z_{in,RF}$ (Ω)
			3.5	4.65	102.85 – j 110.27	37.35 – j 30.84
5.6	0.2	11.4	4.5	3.84	89.39 – j 79.25	33.19 – j 23.37
			5.5	3.9	75.19 – j 58.70	28.59 – j 17.23
			6.5	5.37	62.823 – j 45.20	24.34 – j 12.16

quarter-wave stub. The transmission coefficients ($S21$) of a conventional open-circuit quarter-wave stub are −36 and −0.4 dB at 2 and 4 GHz, respectively. On the other hand, the DBS shows an additional 32-dB suppression at 4 GHz. Worth mentioning is that the length of the stub reduces up to 30%, which implies the circuit size can be much reduced when the SCMRC is introduced. The measured insertion loss is comparable to that of a conventional quarter-wave stub. In addition, the incorporated SCMRC has no adverse effect on the bandwidth.

III. MIXER DESIGN

Fig. 7 shows the schematic diagram of our second SHP mixer. It consists of four parts, i.e.: 1) the antiparallel diode pair and the 2) LO; 3) the RF; and 4) IF networks. The antiparallel diode pair is the nonlinear device for both up- and down-conversion. The LO network provides the return path for the RF (11.2 GHz) and IF (0.2 GHz) signals by two open-short DBSs, and the RF network provides the return path for the LO (5.5 GHz) signal. In addition, both RF and LO networks terminate the idler frequencies (for down-conversion, $2f_{\rm LO} + f_{\rm RF} = 22.2$ GHz, $4f_{\rm LO} + f_{\rm RF} = 33.2$ GHz, $6f_{\rm LO} - f_{\rm RF} = 21.8$ GHz, and $8f_{\rm LO} - f_{\rm RF} = 32.8$ GHz. For up-conversion, $4f_{\rm LO} \pm f_{\rm IF} = 21.8/22.2$ GHz and $6f_{\rm LO} \pm f_{\rm IF} = 32.8/33.2$ GHz) reactively so as to suppress them and dramatically improve the conversion loss. Finally, two shunt radial stubs ($\lambda_{\rm LO}/4$ and $\lambda_{\rm RF}/4$) in the IF network present a short termination for the RF and LO frequencies, respectively, and prevent them from leaking into the IF port.

LO Network: In the LO network, an SCMRC was added into a shunt short-circuit stub such that it can serve as a dual-frequency termination. Open-short DBS is chosen because the dc/IF signal can be shorted and returned directly through this network, thus eliminating an extra IF return path. To enhance the operating bandwidth, another DBS with an identical structure was used. The SCMRC separates the stub into two sections. For the whole

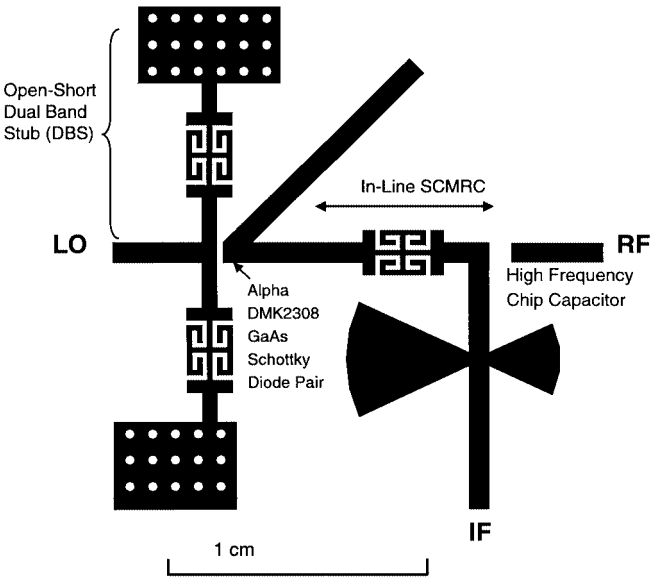

(a)

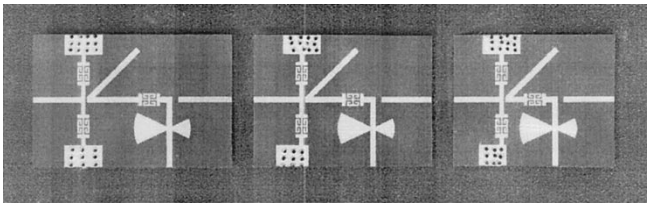

(b)

Fig. 11. Novel second SHP mixer incorporating DBS and in-line SCMRC. (a) Microstrip layout. (b) Photograph of the fabricated microstrip SHP mixer. The average total circuit size is 14.75 mm × 19.64 mm.

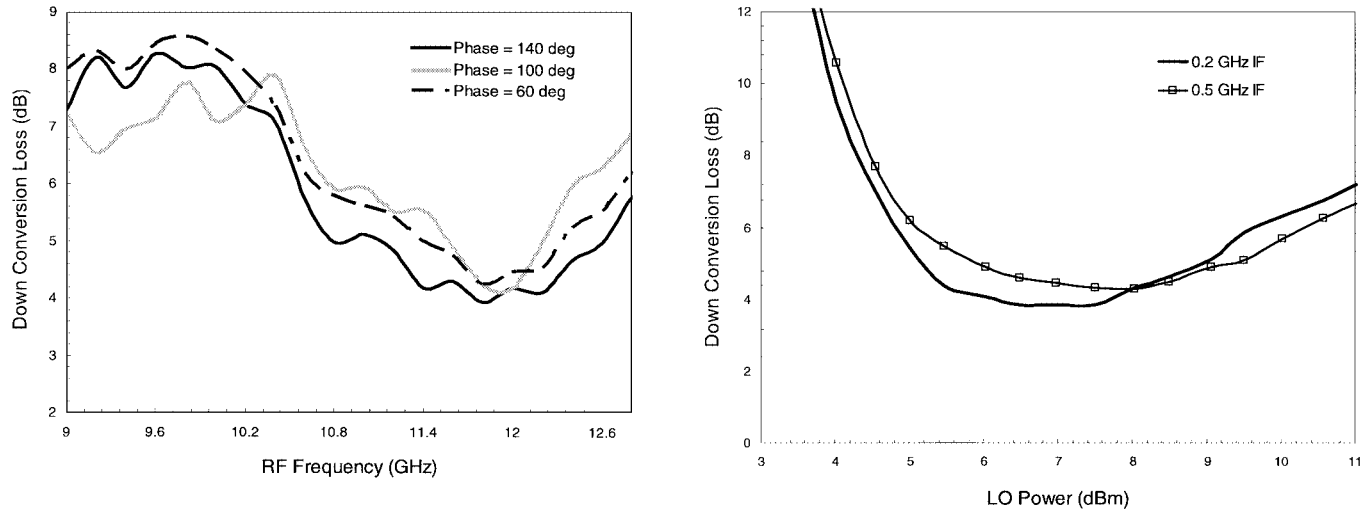

(a) (b)

Fig. 12. Measured SSB down-conversion loss: (a) versus RF frequency at LO power corresponding to 6.5 dBm and (b) versus LO power at an RF frequency of 11.6 GHz (both are 0.2-GHz IF).

section, i.e., L_1, it is electrically tuned as a half-wavelength long at the RF frequency, which grounds the RF. On the other hand, due to the stopband of the SCMRC at one of the idler frequencies (21.8/22.2 GHz), the upper section of these stubs, i.e., L_2, is tuned to be a quarter-wavelength long and serves like an open-circuited quarter-wave shunt stub at these frequencies so as to terminate and suppress them. By incorporating the SCMRC into a single stub, the whole length of the stub reduces by over 50%. Moreover, at IF frequency (0.2 GHz), the length of the stub is negligibly small compared with its wavelength so that the IF signal is grounded directly and a return path is built. Note that the open-short DBS is different from a normal short-circuit stub. This is because the dual-frequency ratio can be tuned independently according to the value of the undesired mixing products, rather than an integral multiple of two. As a result, the DBS design is more flexible and easy to adjust. Indeed, for a lower LO requirement, as well as better conversion-loss performance, an optional LO matching network can be added in this LO network. However, the matching circuits may encounter extra losses, which will mitigate the gains from this network. For simplicity, such a network is omitted in this study. Fig. 8 shows the simulated transmission characteristics ($S21$) and the reflection phases ($S11$) of the LO network. It can be seen that both stopband and short terminations ($\pm 180^\circ$) can be achieved simultaneously at the RF ($\sim$9–11.5 GHz) and the major idler frequency range ($\sim$20–25 GHz).

RF Network: In the RF network, the conventional open-circuit quarter-wave stub presents a short termination and a return path for the LO frequency (5.5 GHz). It should be noted that the following in-line SCMRC is a wide bandstop structure covering both the image and idler frequencies (for down-conversion, the image $2f_{\rm LO} + f_{\rm RF} = 22.2$ GHz, the idler frequencies $4f_{\rm LO} + f_{\rm RF} = 33.2$ GHz, $6f_{\rm LO} - f_{\rm RF} = 21.8$ GHz, and $8f_{\rm LO} - f_{\rm RF} = 32.8$ GHz. For up-conversion, the idler frequencies $4f_{\rm LO} \pm f_{\rm IF} = 21.8/22.2$ GHz and $6f_{\rm LO} \pm f_{\rm IF} = 32.8/33.2$ GHz). By tuning the length (θ_0) of the transmission line between the diode pair and SCMRC (Fig. 7), the cell

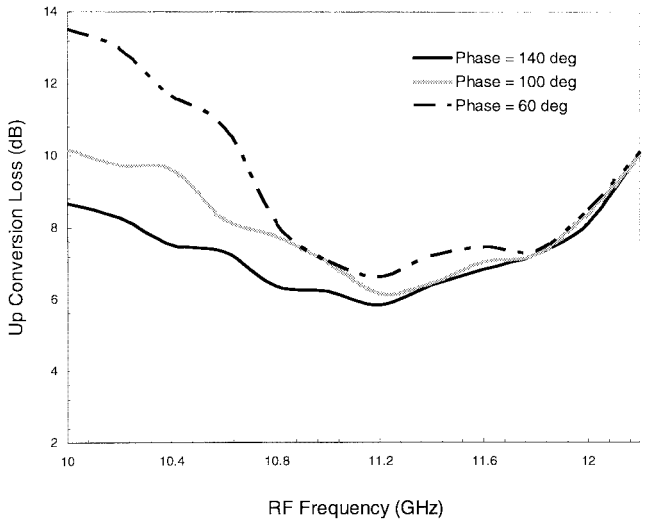

Fig. 13. Measured SSB up-conversion loss versus RF frequency at LO power corresponding to 7 dBm (0.2-GHz IF).

then presents different reflection phases on the right terminal of the diode pair, which satisfies Madjar's design criteria [9] that terminations of the idler frequencies should have an optimized phase to minimize the conversion loss. Therefore, the in-line SCMRC can provide a suitable reactive termination for these idler frequencies and the image, and suppresses them effectively. In addition, since the in-line SCMRC is an excellent transmission line for the IF and RF frequencies, these two frequencies can pass through without any adverse effects. In addition, a high-frequency chip capacitor is placed in the RF network to isolate the IF and RF frequency. This capacitor passes the RF signal, but presents an open circuit for the dc/IF frequency so that dc/IF signal is not loaded by the impedance of the RF port. Fig. 9 shows the simulated transmission characteristics ($S21$) and the reflection phases ($S11$) of this RF network. At approximately 21.5–23 GHz, which is the frequency range of the major idler signals, the phase of $S11$ of this RF network is -90°. In

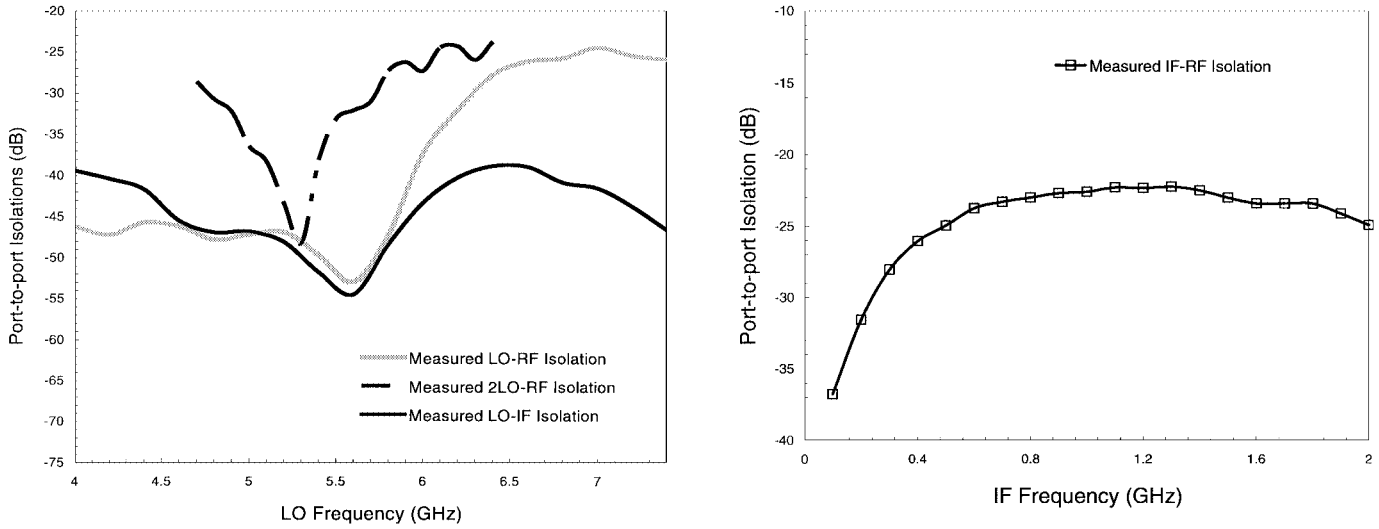

(a) (b)

Fig. 14. Measured port-to-port isolation. (a) LO–RF, 2LO–RF, and LO–IF. (b) IF–RF.

practice, an optimum phase can be tuned according to the optimization of the simulated conversion loss.

IF Network: In the IF network, two open radial stubs (a $\lambda_{\rm RF}/4$ and a $\lambda_{\rm LO}/4$ long radial stub) present a short termination for RF and LO frequencies, respectively, so that the IF port will not degrade the conversion-loss performance by loading the RF and LO signal. The radial stub is chosen because we want to have a wide-band rejection of RF and LO signals in this network. All the components in this network are electrically small at the IF frequency and have no effect on it. Fig. 10 shows the simulated transmission characteristics ($S21$) and reflection phases ($S11$) of this IF network.

In summary, the proposed second SHP mixer works as follows: for up-conversion, the IF signal feeds from the right-hand side of the diode pair and returns through the DBSs at the left-hand side of the diode pair. The in-line SCMRC and quarter-wave stub have no effect on the IF feed signal. The LO signal is fed from the left-hand side of the diode pair and returned through the conventional quarter-wave stub on the right-hand side of the diode pair. The two identical shunt DBSs not only have no effect on the LO feed signal, but also provide a short terminal for the two fundamental idlers $4f_{\rm LO} \pm f_{\rm IF}$ on the left-hand side of the diode pair for their suppression. In addition, an in-line SCMRC with a tunable phase provides a reactive termination for four idlers ($4f_{\rm LO} \pm f_{\rm IF}$ and $6f_{\rm LO} \pm f_{\rm IF}$) on the right-hand side of the diode pair.

For down-conversion, the RF signal pumps from the right-hand side of the diode pair and returns through the two identical shunt DBSs on the left-hand side. Also, the in-line SCMRC and quarter-wave stub have no effect on the RF signal on the right-hand side. Same as up-conversion, the LO signal is fed from the left-hand side and returned through the quarter-wave stub on the right-hand side. The two identical shunt DBSs on the left-hand side not only have no effect on the LO feed signal, but also provide a short terminal for one image $2f_{\rm LO} + f_{\rm RF}$ and one fundamental idler $4f_{\rm LO} + f_{\rm RF}$ on the left-hand side of the diode pair for their suppression. Here,

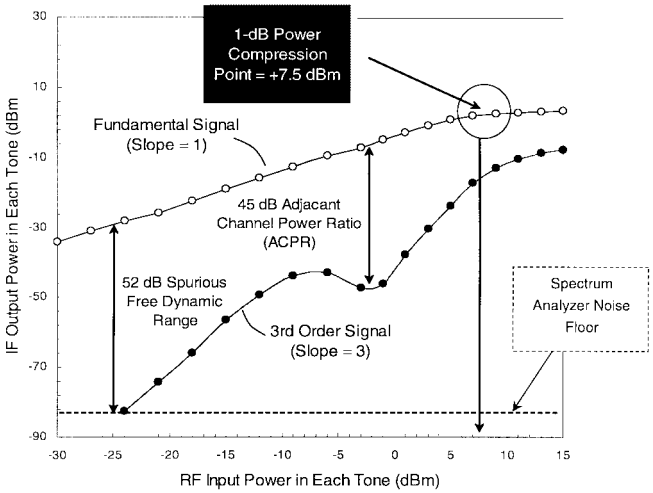

Fig. 15. Output power at the IF port versus the RF input power in each tone. $f_{\rm LO} = 5.6$ GHz, LO power $= +6.5$ dBm, $f_{\rm RF1} = 11.3998$ GHz, $f_{\rm RF2} = 11.4002$.

the in-line SCMRC stub provides a reactive termination for one image $2f_{\rm LO} + f_{\rm RF}$ and three idlers $4f_{\rm LO} + f_{\rm RF}$, $6f_{\rm LO} - f_{\rm RF}$, and $8f_{\rm LO} - f_{\rm RF}$ on the right-hand side of the diode pair. Their combined effect results in a low conversion-loss mixer design.

IV. Fabrication and Measurements

In this paper, *Microwave Office 2000*[2] was used to calculate and optimize the mixer performance through a harmonic balance analysis (HBA) routine. A commercial GaAs flip-chip Schottky diode pair (Alpha DMK2308) was used and bounded to the circuit using silver epoxy. In the simulation, the standard SPICE model for the Schottky diode is employed and its parameters are shown in Table I. The simulation is based on the ideal transmission-line model, which does not include any conductor loss and junction effects. Table II shows the simulated results of the mixer conversion loss and the RF and LO device im-

[2]Applied Wave Res. Inc., El Segundo, CA.

TABLE III
PERFORMANCE COMPARISON WITH OTHER REPORTED MIXERS

Reference	Mixer Topology	Order of LO Harmonics	Frequency Range	LO Power Level (dBm)	Conversion Loss (dB)
[8]	Passive - Antiparallel Diode Pair	2	36 - 40 GHz Up Conversion	6	10
[9]	Passive - Antiparallel Diode Pair	2	27.5 - 31 GHz Up Conversion	---	9
[2]	Passive - Antiparallel Diode Pair	2	22 - 24 GHz Up Conversion	---	10 - 12
[5]	Passive - Antiparallel Diode Pair	2	26 – 36 GHz Down Conversion	11	10.26 – 12.45
[6]	Passive - Antiparallel Diode Pair	2	21.6 - 30.8 GHz Down Conversion	6 - 7	12.4
[26]	Passive - Antiparallel Diode Pair	2	9 - 11 GHz Up Conversion	7	12
[27]	Passive - GaAs MESFET	2	8.45 GHz Down Conversion	6	13
[28]	Passive - Antiparallel Diode Pair	2	5.8 GHz Down Conversion	4	9
This Work	**Passive - Antiparallel Diode Pair**	**2**	**10.5 - 13 GHz**	**6 - 7.5**	**< 6.8 Mini. = 3.9**

pedances. Three optimized circuits with different phases (60°, 100°, and 140°) at the right terminal of the diode pair for terminations of the idlers were then fabricated and measured. Fig. 11 shows the circuit pattern of the second-order SHP mixer, which was built on Duroid5880 with $\varepsilon_r = 2.2$, $h = 0.254$ mm. The average circuit size, excluding the subminiature A (SMA) connectors, is 14.75 mm $\times$ 19.64 mm. These prototypes were then mounted onto a microstrip enclosure with SMA connectors at the RF, LO, and IF ports for testing purposes.

Fig. 12(a) shows the measured single-sideband (SSB) down-conversion loss versus RF frequency at the LO power corresponding to the minimum down-conversion loss. The results were obtained with the IF frequency fixed at 0.2 GHz. At an RF of 11.6 GHz and with an LO power of 6.5 dBm, the measured minimum SSB down-conversion loss is 3.9 dB, which is the best result ever reported for a planar X-band second SHP mixer. Furthermore, it can be seen that when $\theta_0 = 140°$, the mixer is tuned to have a wider bandwidth with the SSB conversion loss of 4.5–5.5 dB from 10.6–12.6 GHz and less than 8.6 dB for the whole measurement range. Fig. 12(b) shows the measured SSB down-conversion loss versus the LO power, in which the RF frequency is fixed at 11.6 GHz. It is found that the lowest conversion loss of the proposed mixer happens at the LO power of 6 dBm and remains stable up to 7.5 dBm.

The mixer circuit was also measured as an up-converter. Measurement setup and the port arrangement are the same as that in the down-conversion. With the IF signal fixed at 0.2 GHz, the SSB measured up-conversion loss for the USB ($f_{\mathrm{RF}} = 2f_{\mathrm{LO}} + f_{\mathrm{IF}}$) versus RF frequency at the LO power (7 dBm) corresponding to the minimum up-conversion loss is shown in Fig. 13. The minimum up-conversion loss is 5.8 dB at 11.2 GHz, and remains below 8.4 dB from 10 to 12 GHz. By setting $\theta_0 = 140°$, both the minimum up-conversion loss and a better bandwidth can be achieved.

Fig. 14 shows the measured port-to-port (LO–RF, 2LO–RF, LO–IF, and IF–RF) isolations. With the IF port terminated by a matched load, the measured LO–RF and 2LO–RF isolations shown in Fig. 14(a) is better then -50 and -40 dB, respectively for LO frequencies of 5.4–5.8 GHz. The LO–RF isolation is expected to remain better than -38 dB from 4 to 6 GHz. The LO–IF isolation was also measured using the same setup, but with the RF port terminated by a matched load. The measured LO–IF isolation remains better than -40 dB for the measured frequency range and has a minimum isolation around 5.6 GHz. Fig. 14(b) shows the measured IF–RF isolation with the LO pumped with the operating power level. The measured IF–RF isolation has a minimum port isolation of -37 dB at 0.1 GHz and generally increases up to around -23 dB.

Linearity is a critical requirement in modern communication systems. The IMD performance of an RF receiver is often limited by that of the mixer. This is especially the case of SHP mixers, which are known to demonstrate a higher distortion [19]. Since the third-order IMDs are located very close to the desired IF signal, these products are the most serious ones to be eliminated [20]–[23]. A good figure-of-merit mixer with lower IMD level and higher 1-dB power compression point (P1dB) is needed in order to achieve a larger dynamic range for the whole receiver system.

The linearity of the mixer prototype has been tested using a standard two-tone RF signals at 11.4002 and 11.3998 GHz, respectively. Fig. 15 plots the IF and IMD3 power in each tone depending upon different RF input power. The 1-dB input power compression point is measured and determined $+7.5$ dBm under the LO level of 6.5 dBm with 52-dB spurious-free dynamic range. The adjacent channel power ratio (ACPR) is approximately 45 dBc lower than the respective IF power at RF power of -3 dBm, which results in a distinctive linearized IMD null and a large dynamic range. It is worth mentioning that such performance normally appears in linearized mixers only. Compared with other linearized mixers reported in the open literature [20]–[23], our proposed design shows a comparable or even better performance, especially for an SHP mixer working up to X-band.

V. Conclusion and Discussion

A low-cost high-performance X-band SHP mixer has been implemented in a planar microstrip structure utilizing our novel SCMRC. The total circuit size excluding the SMA connectors is less than 19.65 mm $\times$ 14.75 mm. The measured minimum SSB down-conversion loss of 3.8 dB at an RF of 11.6 GHz and an IF of 0.2 GHz represents the state-of-the-art performance for a planar X-band SHP mixer, and is even better than a fundamental pumped Schottky diode counterparts. Table III shows the performance of other reported second SHP mixers in the frequency range below 40 GHz for comparison.

The mixer is broad-band with a measured SSB down-conversion loss of less than 8.2 dB over a 9–12.8-GHz measurement range. Moreover, the measured LO–RF isolation is better than -50 dB for LO frequency at 5.8 GHz and is under -30 dB over the LO frequencies range of 4–6.2 GHz, which is extremely important in receiver applications to minimize the leakage of LO power to the RF network. It is not surprising that the prototype is linearized by the proposed design method, resulting in excellent performance for both the 1-dB compression point and the dynamic-range parameters as spurious harmonics are efficiently eliminated. It is expected that the proposed SHP mixer design would find a great potential in low-cost high-performance wireless receiver systems.

Acknowledgment

The authors wish to acknowledge an anonymous reviewer for suggesting the measurement of the linearity response of the proposed design.

References

[1] M. Cohn, J. E. Degenford, and B. A. Newman, "Harmonic mixing with an antiparallel diode pair," *IEEE Trans. Microwave Theory Tech.*, vol. MTT-23, pp. 667–673, Aug. 1975.

[2] F. D. Flaviis, T. Rozzi, F. Moglie, A. Sgreccia, and A. Panzeri, "Accurate analysis and design of millimeter wave mixers," *IEEE Trans. Microwave Theory Tech.*, vol. 41, pp. 870–873, May 1993.

[3] S. D. Vogel, "Design and measurements of a novel subharmonically pumped millimeter-wave mixer using two single planar Schottky-barrier diodes," *IEEE Trans. Microwave Theory Tech.*, vol. 44, pp. 825–831, June 1996.

[4] S. Raman, F. Ruchy, and G. M. Rebeiz, "A high-performance W-band unplanar subharmonic mixer," *IEEE Trans. Microwave Theory Tech.*, vol. 45, pp. 955–958, June 1997.

[5] H. Gu and K. Wu, "A novel uniplanar balanced subharmonically pumped mixer for low-cost broadband millimeter-wave transceiver design," in *IEEE MTT-S. Int. Microwave Symp. Dig*, June 2000, pp. 635–638.

[6] H. Okazaki and Y. Yamaguchi, "Wide-band SSB subharmonically pumped mixer MMIC," *IEEE Trans. Microwave Theory Tech.*, vol. 45, pp. 2375–2379, Dec. 1997.

[7] M. W. Chapman and S. Raman, "A 60 GHz uniplanar MMIC 4$\times$ subharmonic mixer," *IEEE Trans. Microwave Theory Tech.*, vol. 50, pp. 2580–2588, Nov. 2002.

[8] K. Itoh and M. Shimozawa, "Fundamental limitations of conversion loss and output power on an even harmonic mixer with junction capacitance," in *IEEE MTT-S. Int. Microwave Symp. Dig.*, June 2001, pp. 1333–1336.

[9] A. Madjar, "A novel general approach for the optimum design of microwave and millimeter wave subharmonic mixers," *IEEE Trans. Microwave Theory Tech.*, vol. 44, pp. 1997–2000, Nov. 1996.

[10] Q. Xue, K. M. Shum, and C. H. Chan, "Novel 1-D microstrip PBG cells," *IEEE Microwave Guided Wave Lett.*, vol. 10, pp. 403–405, Oct. 2000.

[11] F.-R. Yang, K.-P. Ma, Y. Qian, and T. Itoh, "A uniplanar compact photonic-bandgap (UC-PBG) structure and its applications for microwave circuits," *IEEE Trans. Microwave Theory Tech.*, vol. 47, pp. 1509–1514, Aug. 1999.

[12] T.-Y. Yun and K. Chang, "One-dimensional photonic bandgap resonators and varactor tuned resonators," in *IEEE MTT-S. Int. Microwave Symp. Dig.*, June 1999, pp. 629–632.

[13] C.-K. Wu, H.-S. Wu, and C.-K. C. Tzuang, "Electric-magnetic-electric slow-wave microstrip line and bandpass filter of compressed size," *IEEE Trans. Microwave Theory Tech.*, vol. 50, pp. 1996–2004, Aug. 2002.

[14] F.-R. Yang, Y. Qian, and T. Itoh, "A novel uniplanar compact PBG structure for filter and mixer applications," in *IEEE MTT-S. Int. Microwave Symp. Dig.*, June 1999, pp. 919–922.

[15] K. M. Shum, Q. Xue, and C. H. Chan, "A novel microstrip ring hybrid incorporating a PBG cell," *IEEE Microwave Wireless Comp. Lett.*, vol. 11, pp. 258–260, June 2001.

[16] Q. Xue, K. M. Shum, and C. H. Chan, "Novel oscillator incorporating a compact microstrip resonant cell," *IEEE Microwave Wireless Comp. Lett.*, vol. 11, pp. 202–204, May 2001.

[17] ——, "Low conversion loss fourth subharmonic mixers incorporating CMRC for millimeter-wave applications," *IEEE Trans. Microwave Theory Tech.*, vol. 51, pp. 1449–1454, May 2003.

[18] Q. Xue, Y. F. Liu, K. M. Shum, and C. H. Chan, "A study of compact microstrip resonant cells with applications in active circuits," *Microwave Opt. Technol. Lett*, vol. 31, pp. 81–83, 2001.

[19] S. A. Maas, *Microwave Mixers*. Boston, MA: Artech House, 1993.

[20] Y. Kim, Y. Kim, and S. Lee, "Linearized mixer using predistortion technique," *IEEE Microwave Guided Wave Lett.*, vol. 12, pp. 204–205, June 2002.

[21] M. Chongeheawchamnan and I. D. Robertson, "Linearized microwave mixer using simplified feedforward technique," *Electron. Lett.*, vol. 36, no. 9, pp. 724–725, Apr. 1999.

[22] T. Nesimoglu, M. A. Beach, P. A. Warr, and J. R. Macleod, "Linearised mixer using frequency retranslation," *Electron. Lett.*, vol. 37, no. 25, pp. 1493–1494, Dec. 2001.

[23] F. D. Flaviis and S. A. Maas, "X-band doubly balanced resistive FET mixer with very low intermodulation," *IEEE Trans. Microwave Theory Tech.*, vol. 43, pp. 457–460, Feb. 1995.

[24] A. C. Azevedo Dias, D. Consonni, and M. A. Luqueze, "High isolation sub-harmonic mixer," in *IEEE MTT-S/APS/LEOS Int. Microwave Optoelectronics Conf.*, vol. 2, 1999, pp. 378–381.

[25] K. Mori, H. Arai, Y. Qian, and T. Itoh, "Direct conversion receiver for digital beamforming at 8.45 GHz," in *IEEE MTT-S. Int. Microwave Symp. Dig.*, June 2001, pp. 1375–1378.

[26] S. Lin, Y. Qian, and T. Itoh, "Quadrature direct conversion receiver integrated with planar quasi-Yagi antenna," in *IEEE MTT-S. Int. Microwave Symp. Dig.*, June 2000, pp. 1285–1288.

Tsz Yin Yum (S'02) was born in Hong Kong, in 1980. He received the B.Eng. degree (with first-class honor) in electronic engineering from the City University of Hong Kong, Kowloon, Hong Kong, in 2002, and is currently working toward the M. Phil. degree at the City University of Hong Kong.

His research interests include both microwave active and passive circuit and antenna designs.

Mr. Yum has been the President of the IEEE Student Branch (Hong Kong Section), City University of Hong Kong, since 2003. He was the recipient of the 2000 VTech Scholarship, the 2002 Sir Edward Youde Memorial Fellowship, and the third-place winner of the Student Paper Competition of the 2003 IEEE Microwave Theory and Techniques Society (IEEE MTT-S) International Microwave Symposium (IMS).

Quan Xue (M'02) received the B.S., M.S., and Ph.D. degrees in electronic engineering from the University of Electronic Science and Technology of China, Chengdu, China, in 1988, 1990, and 1993, respectively.

In 1993, he joined the Institute of Applied Physics, University of Electronic Science and Technology of China, as a Lecturer. He became an Associate Professor in 1995 and a Professor in 1997. From October 1997 to October 1998, he was a Research Associate and then a Research Fellow with the Chinese University of Hong Kong. Since June 1999, he has been with the Wireless Communications Research Center, City University of Hong Kong, Kowloon, Hong Kong, where he is currently a Senior Scientific Officer. His research interests include microwave circuits and antennas.

Chi Hou Chan (S'86–M'86–SM'00–F'02) received the Ph.D. degree in electrical engineering from the University of Illinois at Urbana-Champaign, in 1987.

Since April 1996, he has been with the Department of Electronic Engineering, City University of Hong Kong, Kowloon, Hong Kong, where he is currently a Chair Professor of electronic engineering, Associate Dean of the Faculty of Science and Engineering, and the Director of the Co-operative Education Center. He is a Guest Professor with Xi'an Jiaotong University, Wuhan University, and Southeast University. He is also an Advisory Professor with the Nanjing University of Science and Technology, Nanjing, China, and an Adjunct Professor with the University of Electronic Science and Technology, China, and Peking University, Beijing, China. His research interests include computational electromagnetics, antenna design, and microwave and millimeter-wave communications systems.

Prof. Chan was a recipient of the 1991 U.S. National Science Foundation (NSF) President Young Investigator (PYI) Award.